
# Three-Dimensional Nuclear Analysis for the HIBALL Reactor Cavity

M.E. Sawan, L.A. El-Guebaly, and W.F. Vogelsang

September 1981

UWFDM-441

Trans. ANS 39 (9181) 780.

FUSION TECHNOLOGY INSTITUTE

UNIVERSITY OF WISCONSIN

MADISON WISCONSIN

# Three-Dimensional Nuclear Analysis for the HIBALL Reactor Cavity

M.E. Sawan, L.A. El-Guebaly, and W.F. Vogelsang

Fusion Technology Institute
University of Wisconsin
1500 Engineering Drive
Madison, WI 53706

http://fti.neep.wisc.edu

September 1981

UWFDM-441

Trans. ANS 39 (9181) 780.

# Three-Dimensional Nuclear Analysis for the HIBALL Reactor Cavity

M. E. Sawan

L. A. El-Guebaly

W. F. Vogelsang

## Abstract

A detailed three-dimensional Monte Carlo nuclear analysis is presented for the HIBALL reactor cavity. The overall tritium breeding ratio and the overall energy multiplication are 1.25 and 1.274, respectively. Nuclear heating in the vacuum pumps was found to be insignificant. The total thermal power for the HIBALL power plant is 10,193 MW(th).

## I. Introduction

A new approach to inertial confinement fusion that is drawing increasing attention is the use of accelerated heavy ions as a fusion target driver. The interaction of heavy ion beams with matter is thought to be better understood than the interaction of laser or electron beams with matter. Furthermore, the coupling efficiency of heavy ions with the fusion target is higher than that for photons or electrons.[1] In addition, heavy ion accelerators have higher efficiencies and greater reliability than large laser systems. Another advantage of the heavy ion beam fusion reactor concept is the possibility of attaining high pulse repetition rate without a severe penalty in capital investment.[2]

A conceptual design for a heavy ion beam driven fusion power plant (HIBALL) has been presented.[3] HIBALL (Heavy Ion Beams and Lithium-Lead) utilizes 4 reactor chambers, each fired at a repetition rate of 5 Hz from a single RF-linac. The beam ions are $Bi^{++}$ at 10 GeV and the total energy of each pulse is 4.8 MJ. This energy is delivered to the target by 20 beams. The targets are made from Pb and PbLi surrounding a cryogenic layer of deuterium and tritium. The 4.8 MJ pulse of $Bi^{++}$ ions is assumed to give a target gain of 83 and a total DT yield of 400 MJ. The first metallic wall, made of the ferritic steel alloy HT-9, is protected from the target X-rays, ion debris, and neutrons by an array of porous SiC tubes through which $Pb_{83}Li_{17}$ coolant/breeder flows. This protection concept is called the INPORT concept, for Inhibited Flow-Porous Tube Concept.[4] The reactor cavity is an upright cylinder with a wedge shaped top.

Neutronics and photonics calculations are required to determine the important fusion reactor parameters such as tritium breeding, nuclear heating,

and radiation damage. In an inertial confinement fusion reactor, neutron interactions with the highly dense fusion target result in neutron spectrum softening, neutron multiplication, and gamma generation. A consistent nuclear analysis must, therefore, account for neutron target interactions. Detailed neutronics and photonics calculations were performed for the HIBALL target.[5] The average energy of emerging neutrons was found to be 11.98 MeV. A target neutron multiplication of 1.046 was obtained. The average energy of gamma photons emerging from the target was found to be 1.533 MeV. The spectra of neutrons and gammas emerging from the target were used as a source for subsequent reactor cavity nuclear analysis. A one-dimensional spherical geometry analysis was performed to determine the optimum blanket design which gives the highest possible energy multiplication with adequate tritium breeding.[3] A packing fraction of 0.33 was chosen for the INPORT tubes which occupy a 2 m thick region in front of the first wall. The effective 66 cm thickness of the INPORT blanket was found to significantly reduce the radiation damage in the first structural wall, allowing it to last for the reactor lifetime.[6]

While the one-dimensional spherical geometry calculations are useful for survey studies and predicting conditions at the reactor midplane, they are not capable of adequately modeling the HIBALL reactor in which a point source exists at the center of a cylindrical reactor cavity with a wedge shaped top blanket and a $Pb_{83}Li_{17}$ pool at the bottom. Furthermore, the HIBALL blanket/shield system is required to accommodate large penetrations for vacuum pumping that cannot be modeled in a one-dimensional analysis. These geometrical effects are expected to have an impact on the system's overall tritium breeding and nuclear heating characteristics. In this work, a three-dimensional

nuclear analysis which adequately models the HIBALL reactor cavity is presented.

## II. Reactor Geometrical Model and Method of Calculation

Figure 1 shows a cross section of the HIBALL reactor cavity. The cavity is an upright cylinder with internal dimensions of 11.5 m height on axis and 10 m in diameter. In the vertical sides of the cavity, the blanket consists of a 2 m thick and 10 m high zone of INPORT tubes. The INPORT tubes have a packing fraction of 0.33 with $Pb_{83}Li_{17}$ occupying 98 v/o of the tubes and the remaining 2 v/o occupied by SiC. The tube support structure is made of HT-9 and occupies 0.7 v/o of the tube region. The top of the cavity has 30 wedge shaped blanket modules. These modules are 50 cm thick and consist of 97 v/o $Pb_{83}Li_{17}$, 1 v/o HT-9, and 2 v/o SiC. Figure 2 shows several views of an upper blanket module. The cross sections show details of the structural frame and the SiC fabric which surrounds the frame entirely. The coolant circulates through these modules and exits through a tube which connects with the radial blanket. The coolant from the upper blanket then drains through the back tubes of the radial blanket. The $Pb_{83}Li_{17}$ in the region connecting the top blanket with the INPORT tubes helps protect the HT-9 structure between the vacuum ducts. The bottom of the cavity has a 1 m deep $Pb_{83}Li_{17}$ pool.

The first metallic wall is 1 cm thick and is made of HT-9. The side wall is 12 m high. The top liner is 7 and 6 m above the midplane at reactor centerline and side wall, respectively. A 40 cm thick reflector consisting of 90 v/o HT-9 and 10 v/o $Pb_{83}Li_{17}$ is used. A 40 cm thick reflector is used at the bottom with holes to allow the coolant to drain out. A catch basin then directs the flow to an outlet tube through which it is pumped to the steam

Figure 1

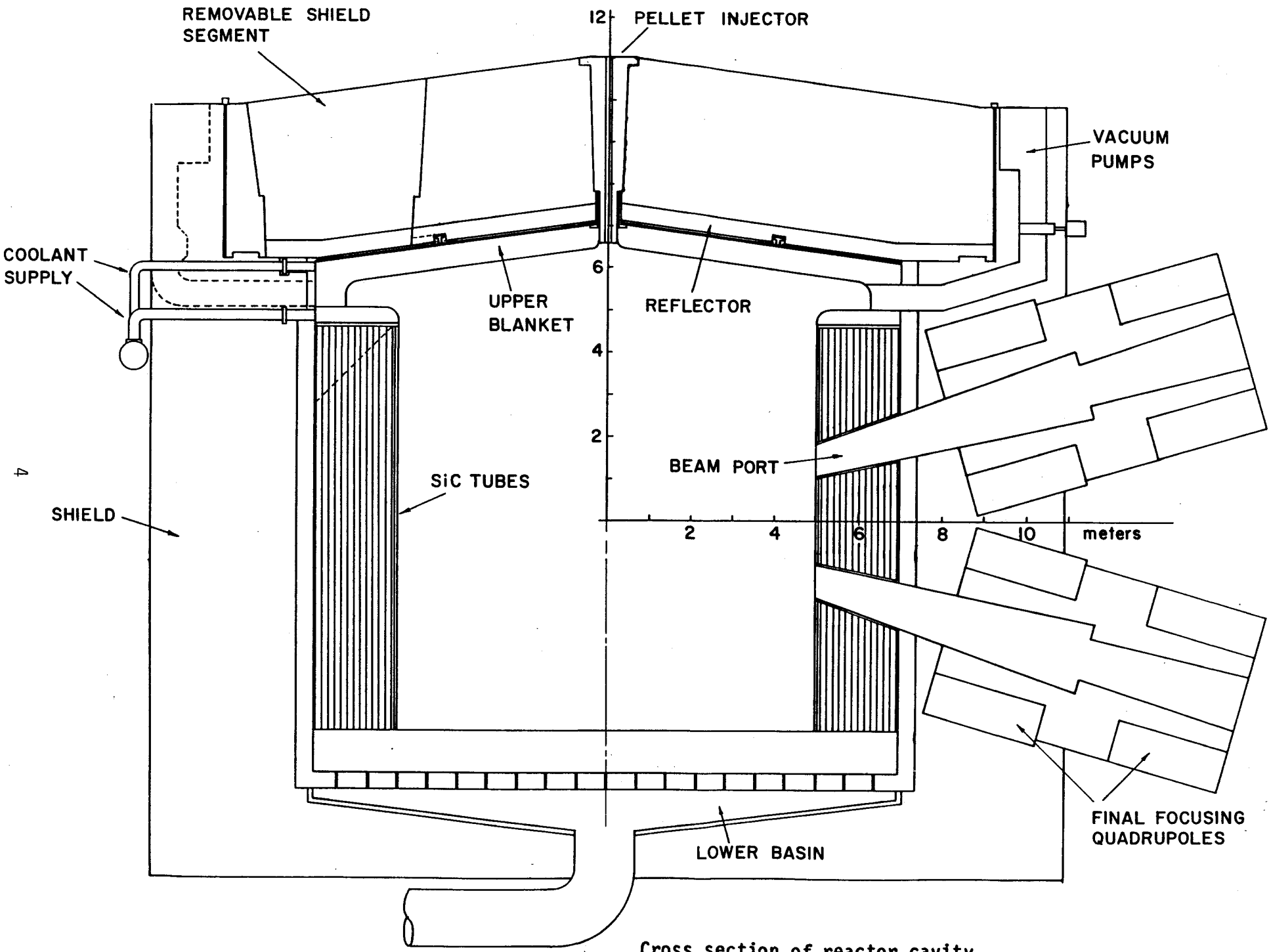


Cross section of reactor cavity.

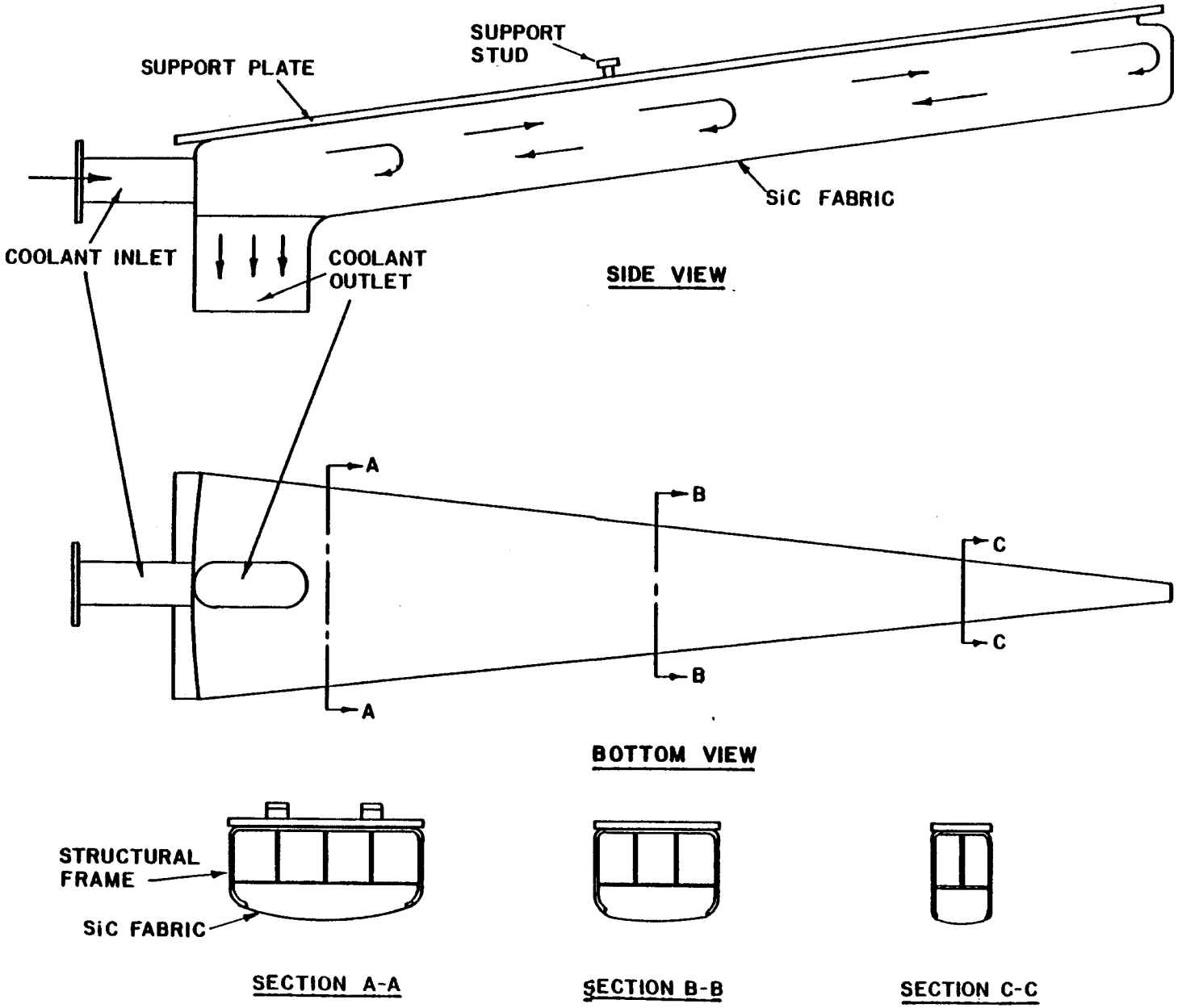


Figure 2 Design of an upper blanket module.

generator. A 3.5 m thick biological shield made of 95 v/o ordinary concrete and 5 v/o water coolant surrounds the reactor.

At the junction between the top blanket modules and the INPORT tubes, there are 30 vacuum system ports, 0.6 m high and 1 m wide. The vacuum ducts, which are concealed from direct line of sight of neutrons, lead to pumping stations located in the upper corner of the reactor cavity. These pumps are used to evacuate the cavity prior to operation and to pump the non-condensable gases.

There are 20 beam ports in each cavity. Each two beams come in at ±16° to the horizontal, spaced at 36° circumferentially. At the first (5 m radius) the total area of the 20 beam ports is 3.6 $m^2$ implying that these penetrations occupy only ~1% of the blanket volume. This is smaller than the statistical uncertainty in the results obtained in the Monte Carlo calculations used in this analysis. Hence, the beam line penetrations are not modeled in the present analysis. Detailed radiation shielding analysis for the beam line penetrations was presented elsewhere.[7] The penetration for target injection in the chamber top is very small and is not considered in this analysis.

The neutronics and photonics calculations were performed using the multi-group three-dimensional Monte Carlo code MORSE.[8] A coupled 25 neutron-21 gamma group cross section library was used. The library consists of the RSIC DLC-41B/VITAMIN-C data library[9] and the DLC-60/MACKLIB-IV response data library.[10] The combinatorial geometry capability of the MORSE code was used to model the problem geometry. Volume detectors were used to estimate the quantities of interest in the different reactor zones. The results presented here are based on a DT yield of 400 MJ and a repetition rate of 5 Hz yielding $7.1 \times 10^{20}$ fusion neutrons per second. A point isotropic source was used at

the center of the reactor cavity with neutron and gamma spectra obtained from the target neutronics and photonics calculations. 4000 histories were used in the Monte Carlo calculations yielding less than 2% statistical uncertainties in the estimates for the tritium breeding ratio and the energy multiplication.

Because of symmetry, only 1/60 of the reactor was modeled with reflecting albedo boundaries used at the planes of symmetry. This corresponds to a "pie slice" with an azimuthal angle of 6°. The geometry for the computational model used is given in Fig. 3. To quantify nuclear heating in the vacuum pump, a 2 cm thick region consisting of 50 v/o 316 SS and 50 v/o Cu is designated as zone 13 to simulate the cryopanels. Zones 14 and 15 represent inner and outer vacuum regions, respectively.

## III. Scalar Flux

Table 1 gives the average neutron and gamma scalar fluxes in the different zones. The fractional standard deviation based on a 68% confidence interval is also included. It is clear from the results that the fractional standard deviation is very small in the breeding blanket zones and is relatively large in the optically thin regions such as the first wall. The results show that while the gamma flux is about two orders of magnitude less than the neutron flux in the breeding blanket zones, it is only one order of magnitude less than the neutron flux in the reflector zones. This results from the large gamma production following neutron capture in the HT-9 structure.

## IV. Tritium Production

Table 2 shows the results for tritium production per DT fusion reaction in the different reactor zones. The contributions from $^{6}Li(n,\alpha)$ and $^{7}Li(n,n'\alpha)$ reactions are shown separately. It is clear that the contribution

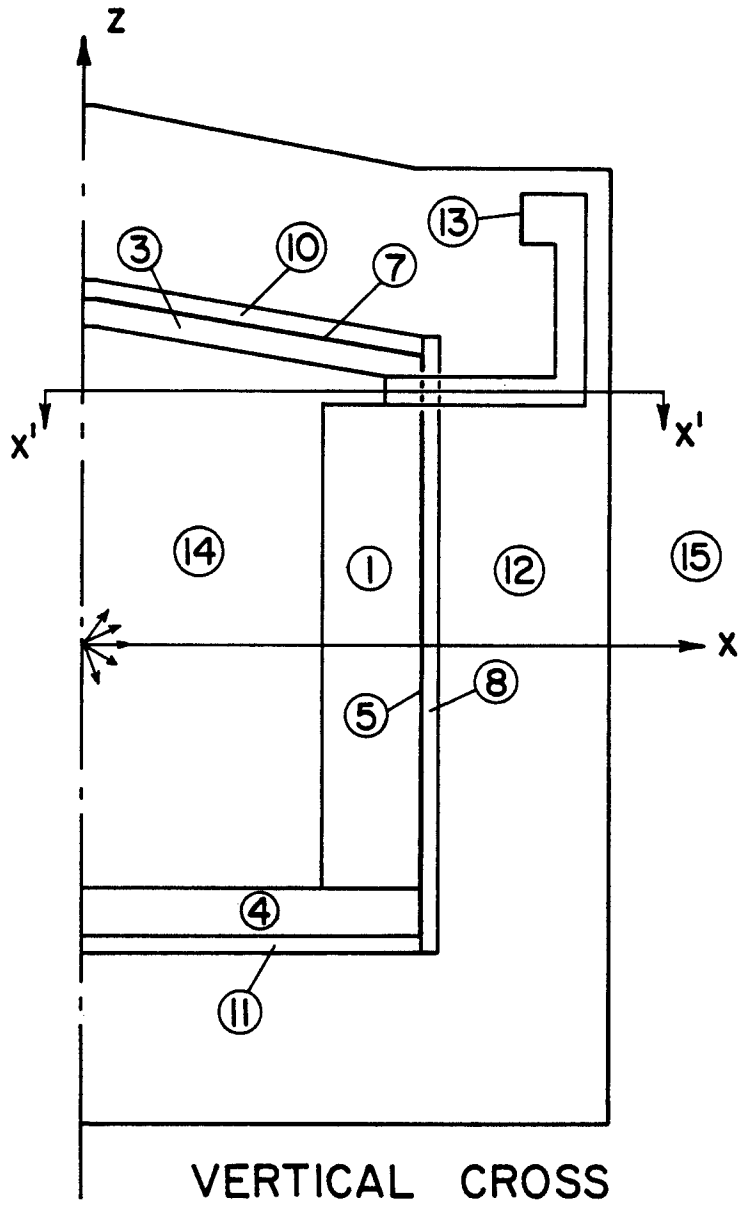


VERTICAL CROSS SECTION AT PLANE y=0

| ZONE | DESCRIPTION |
|---|---|
| 1 | INPORT TUBES |
| 2 | BLANKET REGION AT VACUUM DUCT |
| 3 | TOP BLANKET |
| 4 | BOTTOM LiPb POOL |
| 5 | SIDE WALL |
| 6 | WALL AT DUCT |
| 7 | TOP LINER |
| 8 | SIDE REFLECTOR |
| 9 | REFLECTOR AT DUCT |
| 10 | TOP REFLECTOR |
| 11 | BOTTOM REFLECTOR |
| 12 | BIOLOGICAL SHIELD |
| 13 | VACUUM PUMP |

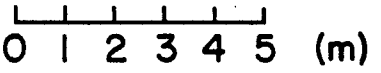


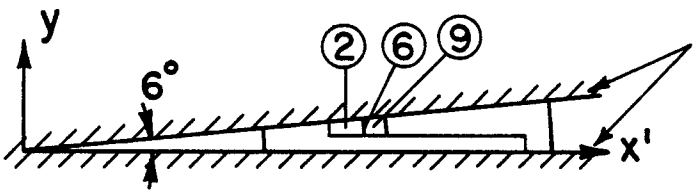


CROSS SECTION x'x'

Figure 3 HIBALL geometry for Monte Carlo calculations.

Table 1 Average Scalar Flux (Particles/$cm^2$/Fusion)

| Region | Zone Number | Neutrons | Gammas |
|---|---|---|---|
| Breeding Blanket | 1 | 3.191(-6) [.015]* | 3.237(-8) [.026] |
| | 2 | 1.691(-6) [.071] | 4.453(-9) [.349] |
| | 3 | 2.937(-6) [.023] | 2.448(-8) [.056] |
| | 4 | 1.708(-6) [.043] | 1.108(-8) [.068] |
| First Wall | 5 | 8.302(-7) [.041] | 2.529(-8) [.118] |
| | 6 | 9.282(-7) [.181] | 1.124(-8) [.600] |
| | 7 | 1.340(-6) [.047] | 4.328(-8) [.164] |
| Reflector | 8 | 2.384(-7) [.034] | 1.274(-8) [.048] |
| | 9 | 4.470(-7) [.153] | 3.213(-8) [.245] |
| | 10 | 3.789(-7) [.044] | 2.230(-8) [.070] |
| | 11 | 8.354(-8) [.126] | 3.739(-9) [.132] |

*Fractional Standard Deviation

Table 2 Tritium Production (Tritons/Fusion)

| Region | Zone Number | $^{6}Li(n,\alpha)T$ | $^{7}Li(n,n'\alpha)T$ |
|---|---|---|---|
| Breeding Blanket | 1 | 0.729 | 0.018 |
| | 2 | 0.014 | 0.00001 |
| | 3 | 0.212 | 0.004 |
| | 4 | 0.235 | 0.004 |
| | Region Total | 1.190 | 0.026 |
| Reflector | 8 | 0.022 | 0.000002 |
| | 9 | 0.001 | 0.0000001 |
| | 10 | 0.009 | 0.000002 |
| | 11 | 0.002 | 0.0000001 |
| | Region Total | 0.034 | 0.000004 |
| System Total | | 1.224 | 0.026 |

from $^{7}Li$ represents ~ 2% of the total tritium production in the breeding blanket region. The reason is that the number of Pb(n,2n) reactions occurring in the $Pb_{83}Li_{17}$ blanket is much larger than that of $^{7}Li(n,n'\alpha)$ reactions. The resulting (n,2n) neutrons are well below the threshold energy for $^{7}Li(n,n'\alpha)$ reaction and hence can produce tritium only through the $^{6}Li(n,\alpha)$ reaction. In the reflector region, the $^{7}Li$ contribution to tritium production is very small because of the neutron spectrum softening in the breeding blanket. Figure 4 gives the spatial distribution of tritium production in the reactor midplane. The contribution from $^{7}Li$ decreases sharply as one moves from the first surface towards the back of the blanket because of the increased neutron spectrum softening.

We notice that as much tritium production occurs in the top blanket as in the bottom $Pb_{83}Li_{17}$ pool, even though the top blanket is only half as thick as the bottom pool and includes 1 v/o HT-9 structure. The reason in that the 2 v/o SiC present in the top blanket enhances neutron slowing down and hence increases the tritium breeding effectiveness. In fact, our results show that the breeding capability of $Pb_{83}Li_{17}$ can be improved considerably by enriching Li and/or using moderators in the blanket. The improvement in systems using $Pb_{83}Li_{17}$ is much more pronounced than that in systems using other breeding materials because most of the contribution to breeding in the $Pb_{83}Li_{17}$ case comes from the $^{6}Li(n,\alpha)$ reaction which has a 1/v cross section in the low energy region.

The overall tritium breeding ratio is found to be 1.25. The confidence interval for the estimated breeding ratio is 0.025 which is 2% of the obtained estimate. The overall tritium breeding ratio obtained here with the actual reactor cavity cylindrical geometry is ~ 5% larger than that obtained from the

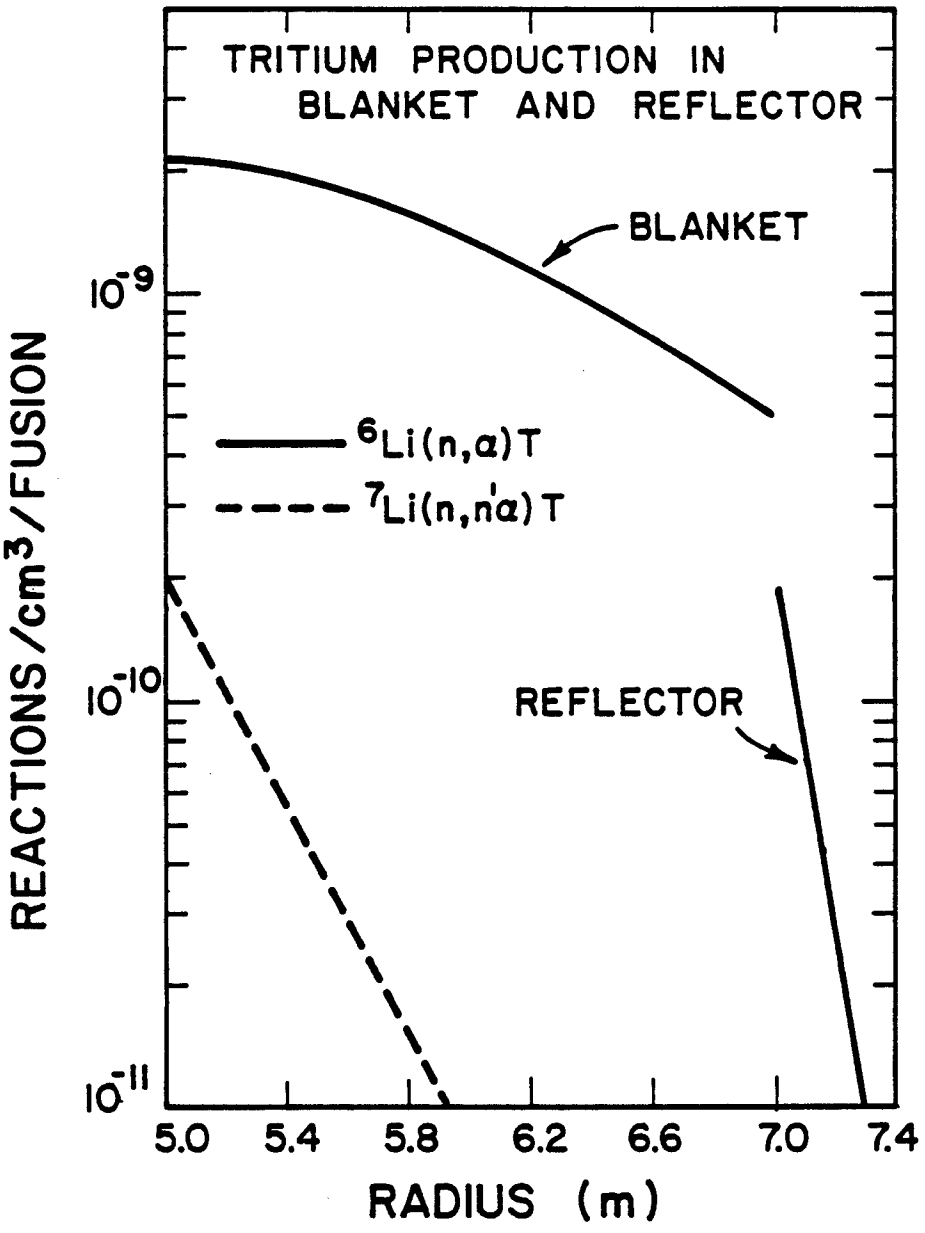


Figure 4 Tritium production in the blanket and reflector.

one-dimensional spherical geometry calculations (1.195). The reason is that in the spherical geometry case, all source neutrons are incident on the blanket perpendicularly to its inner surface and hence will see the same blanket thickness. On the other hand, the source neutrons emitted isotropically at the center of the cylindrical cavity impinge on the inner surface of the blanket at different angles and hence will see larger blanket thicknesses. In other words, the neutron source is surrounded by a larger volume of breeding material in the actual cylindrical case as compared to the case of an equivalent spherical blanket.

## V. Nuclear Heating

Table 3 shows the nuclear energy deposition for neutrons and gammas in the different zones. The average power density is also included. It is clear that the contributions from neutron and gamma heating are nearly the same in the breeding blanket while the gamma contribution in the first wall and reflector is about an order of magnitude higher than the neutron contribution. This results from gamma generation in the HT-9 structure. About 60% of the total reactor thermal power comes from gamma heating. The energy deposited in the biological shield is 0.06 MeV/fusion which corresponds to a power of 6.82 MW. This represents only 0.27% of the total reactor thermal power. Only the energy deposited in the blanket, first wall, and reflector is considered as recoverable energy. The total recoverable neutron and gamma energy in the reactor per DT fusion is 17.553 ± .292 MeV which is slightly less than that obtained for an equivalent spherical reactor (17.95 MeV). The reason is that more tritium production is obtained in the cylindrical case with less neutrons being captured in the HT-9 structure. A neutron absorbed in $^{6}Li$ releases ~ 4.8 MeV while if it is captured in the HT-9 structure ~ 7

Table 3 Nuclear Heating

| Region | Zone Number | Energy Deposition (MeV/fusion) | | Average Power Density ($W/cm^3$) |
|---|---|---|---|---|
| | | Neutrons | Gammas | |
| Breeding Blanket | 1 | 4.806 | 4.839 | 4.409 |
| | 2 | 0.074 | 0.017 | 3.911 |
| | 3 | 1.339 | 1.147 | 3.515 |
| | 4 | 1.430 | 1.007 | 1.800 |
| | Region Total | 7.649 | 7.010 | 4.409 |
| First Wall | 5 | 0.004 | 0.050 | 1.222 |
| | 6 | 0.0001 | 0.0004 | 2.010 |
| | 7 | 0.003 | 0.039 | 3.068 |
| | Region Total | 0.007 | 0.089 | 1.653 |
| Reflector | 8 | 0.155 | 1.628 | 0.939 |
| | 9 | 0.007 | 0.066 | 1.020 |
| | 10 | 0.070 | 0.733 | 1.465 |
| | 11 | 0.013 | 0.126 | 0.257 |
| | Region Total | 0.245 | 2.553 | 0.941 |
| System Total | | 7.901 | 9.652 | 3.345 |

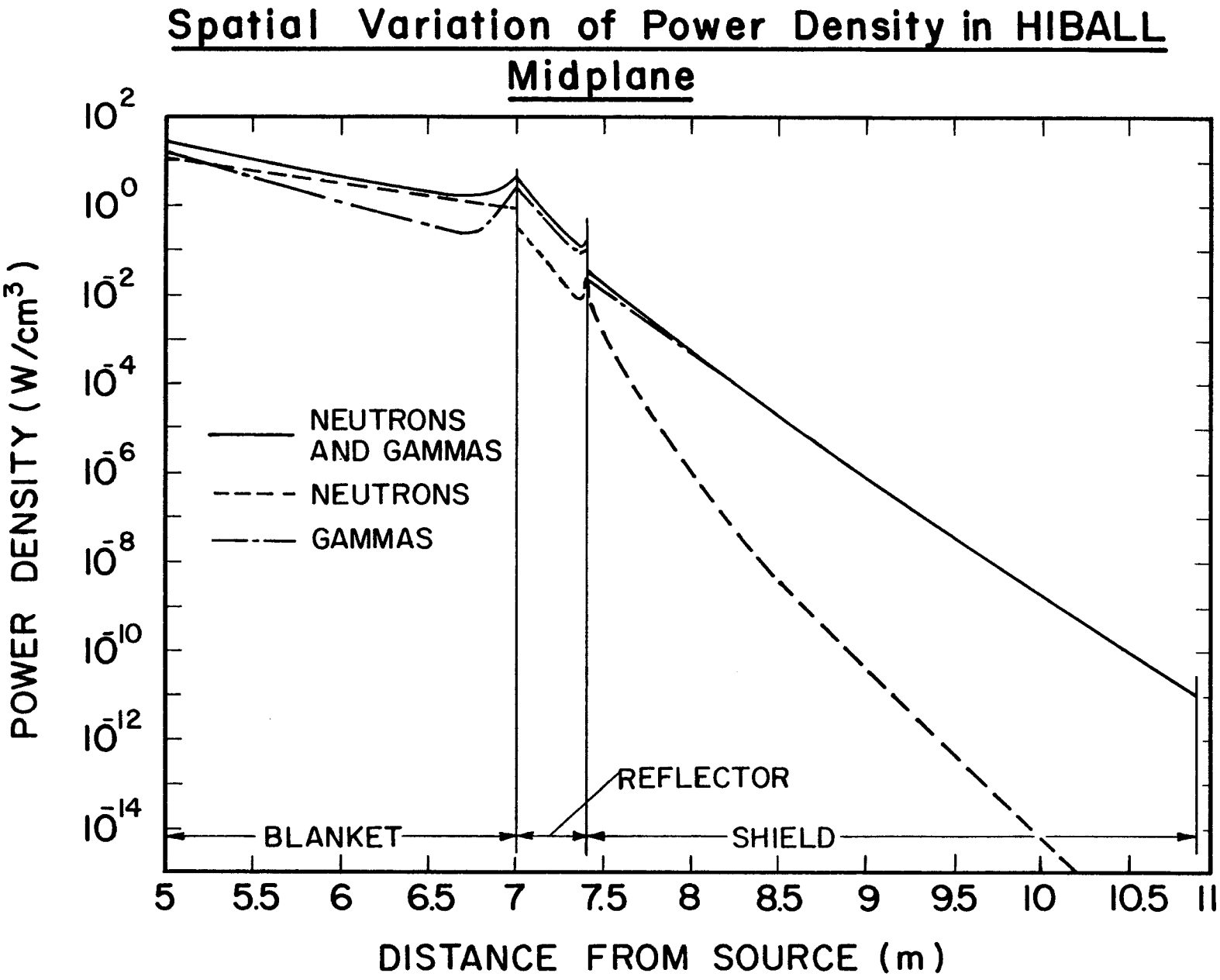


**Figure 5** Spatial variation of power density at HIBALL midplane.

MeV is released. Figure 5 shows the spatial variation of power density in the reactor midplane.

In order to get a statistically adequate estimate of nuclear heating in the vacuum pump with a reasonable number of histories, a Monte Carlo calculation with an angular source biasing was performed. In this run, 4000 histories were used. A volumetric nuclear heating rate of $6 \times 10^{-11}$ W/cm$^3$ was obtained in the vacuum pump (zone 13). The fractional standard deviation was 0.25. Because the vacuum ducts do not see direct line-of-sight source neutrons and they are bent twice, neutron streaming through the ducts was found not to pose any serious problem to the vacuum pump.

The energy flow for the HIBALL fusion reactor design is illustrated in Fig. 6. The target calculations show that the nuclear heating in the target is 1.362 MeV per fusion which when added to the 3.5 MeV alpha particle energy results in a total energy of 4.862 MeV/fusion being carried by the emerging X-rays and ion debris. The energy carried by emerging neutrons and gammas is 12.532 and 0.027 MeV/fusion, respectively. The remaining 0.179 MeV is lost in endoergic neutron reactions. The values given for the power correspond to one reactor cavity. Therefore, these values need to be multiplied by 4 to calculate the power from the whole power plant. This corresponds to a total power plant thermal power of 10,193 MW(th). The overall energy multiplication, defined as the total energy deposited in the system, including the energy deposited by X-rays and target debris at the first surface of the blanket, divided by the fusion reaction yield of 17.6 MeV, is found to be 1.274.

## VI. Summary

A three-dimensional Monte Carlo neutronics and photonics analysis was performed for the HIBALL reactor cavity. An overall tritium breeding ratio of

Figure 6

## ENERGY FLOW IN HIBALL

### HIB PULSE

(4.8 MJ)

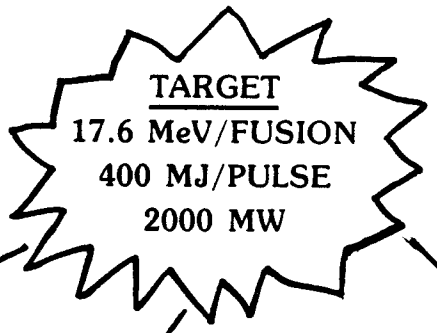


| NEUTRON & GAMMA | X-RAY & DEBRIS | LOST IN ENDOERGIC REACTIONS |
|---|---|---|
| 12.559 MeV | 4.862 MeV | 0.179 MeV |
| 285.42 MJ | 110.49 MJ | 4.08 MJ |
| 1427.1 MW | 552 MW | 20.35 MW |

| | NEUTRON & GAMMA | X-RAY & DEBRIS | TOTAL | |
|---|---|---|---|---|
| BREEDING BLANKET | 14.659 MeV<br>333.16 MJ<br>1667.5 MW | 4.862 MeV<br>110.49 MJ<br>552 MW | 19.521 MeV<br>443.65 MJ<br>2219.5 MW (87.05%) | |
| WALL | 0.096 MeV<br>2.24 MJ<br>10.8 MW | | 0.096 MeV<br>2.24 MJ<br>10.8 MW (0.42%) | 22.415 MeV<br>509.39 MJ<br>2548.3 MW |
| REFLECTOR | 2.798 MeV<br>63.5 MJ<br>318.0 MW | | 2.798 MeV<br>63.5 MJ<br>318.0 MW (12.53%) | |

OVERALL ENERGY MULTIPLICATION = 1.274

1.25 and an overall energy multiplication of 1.274 were obtained. The tritium breeding ratio is higher than that for the equivalent spherical reactor cavity. Nuclear heating in the vacuum pump was found to be very small. The power in the biological concrete shield represents only 0.27% of the total reactor thermal power. The thermal power for the HIBALL power plant is 10,193 MW(th).

Acknowledgment

Support for this work has been provided by the Kernforschungszentrum Karlsruhe and the Bundesministerium für Forschung und Technologie, Federal Republic of Germany, under research agreement with Fusion Power Associates, Gaithersburg, MD.

## References


1. L. Booth and L. Leonard, Trans. Am. Nucl. Soc., 34, 58 (1980).

2. J. Pendergrass et al., Trans. Am. Nucl. Soc., 34, 40 (1980).

3. B. Badger et al., "HIBALL - A Conceptual Heavy Ion Beam Driven Fusion Reactor Study," University of Wisconsin Fusion Engineering Program Report UWFDM-450 (1981).

4. G.L. Kulcinski et al., "The INPORT Concept - An Improved Method to Protect ICF Reactor First Walls," University of Wisconsin Fusion Engineering Program Report UWFDM-426 (August 1981).

5. M.E. Sawan, W.F. Vogelsang, and G.A. Moses, "Coupled Target-Blanket Neutronics and Photonics Analysis for the University of Wisconsin Heavy Ion Beam Fusion Reactor Design," University of Wisconsin Fusion Engineering Program Report UWFDM-395 (1980).

6. M. Sawan, G. Moses, and G. Kulcinski, Trans. Am. Nucl. Soc., 38, 574 (1981).

7. M. Sawan, W. Vogelsang, and D.K. Sze, Trans. Am. Nucl. Soc., 39 (1981).

8. RSIC Code Package CCC-203, "MORSE-CG," Radiation Shielding Information Center, ORNL.

9. RSIC Data Library Collection, "VITAMIN-C, 171 Neutron, 36 Gamma-Ray Group Cross Sections Library in AMPX Interface Format for Fusion Neutronics Studies," DLC-41, ORNL.

10. RSIC Data Library Collection, "MACKLIB, 171 Neutron, 36 Gamma-Ray Group Kerma Factor Library," DLC-60, ORNL.